Journal of Hydrology: Regional Studies 32 (2020) 100764

Contents lists available at ScienceDirect

Journal of Hydrology: Regional Studies

journal homepage: www.elsevier.com/locate/ejrh

From at-site to regional assessment of environmental flows and environmental flows variability in a Mediterranean environment

A. Longobardi [a,*], P. Villani [a,b]

[a] Department of Civil Engineering, University of Salerno, 84084, Fisciano, SA, Italy
[b] CUGRI – InterUniversity Centre for the Prediction and Prevention of Major Hazards, 84084, Fisciano, SA, Italy

ARTICLE INFO

Keywords:
Environmental flows
Flow duration curve
Q_{95}
Regional analysis
Mediterranean area

ABSTRACT

Study region: Data from 28 streamflow gauging stations located in the Campania Region, Southern Italy, were analysed.
Study focus: The study was aimed at recommend regional methodologies for environmental flow (EF) and EF variability estimation for a climatological environment particularly affected by strong climate variability. Starting from an at-site statistical analysis of discharge data, a preliminary step where the quantification of EF average value, $\mu(Q_{95})$, and inter-annual variability, $CV(Q_{95})$, was illustrated. A regional regression approach was then presented for the prediction of $\mu(Q_{95})$ and $CV(Q_{95})$.
New hydrological insights for the region: A step wise procedure highlighted the dominant hydrological variables and catchment attributes for EF prediction. Catchment area and mean annual daily discharge $\mu(Q)$ appeared strongly related to $\mu(Q_{95})$ whereas $CV(Q_{95})$ was found to be dependent on the baseflow index and on precipitation variability. Regional predictions were evaluated on the base of the correlation coefficient and absolute average percentage errors. Prediction errors amounted to about 30 % and 17 % respectively in the case of $\mu(Q_{95})$ and $CV(Q_{95})$. In the end, an implication for a fully regional approach, simply based on catchment attributes, also embedding the impact of hydrological variables, was presented. It showed clearly different performance capacity compared to the prediction based on the observed hydrological variables but not significantly lower.

1. Introduction

Water scientists and stakeholders are nowadays involved in the major challenge of providing the worldwide growing population with reliable water supplies, protecting, at the same time, the ecological integrity of freshwater ecosystems. On this purpose, environmental flow (EF) appears as a critical parameter to be assessed in order to sustain or restore ecosystems and to maintain ecosystem services.

According to Tharme (2003), EF estimating methodologies can be classified into four different groups. It is possible to distinguish between: (i) hydrological methods, based on the analysis of historical flow regime, (ii) hydraulic methods, based on the analysis of stream channel geometry, (iii) habitat simulation methods, based on the simulation of physical habitat, (iv) and holistic methodologies, where multidisciplinary expertise is needed to achieve particular ecological, geomorphological, water quality, social objectives

* Corresponding author at: Via Giovanni Paolo II, 132, 84084, Fisciano, SA, Italy.
E-mail address: alongobardi@unisa.it (A. Longobardi).

https://doi.org/10.1016/j.ejrh.2020.100764
Received 11 June 2020; Received in revised form 27 August 2020; Accepted 11 November 2020
Available online 1 December 2020

in the modified system. The choice for one of the methodologies depends on available data but also on institutional aspects and regulations and thus may vary from country to country. Almost all of these methodologies were criticised because of subjectivity, arbitrariness, or incompleteness and, as far as they actually represent complementary methodologies, a clear trend oriented toward the use of hydrological and combined methods has consolidated over time and over a global scale (Tharme, 2003; Alcázar and Palau, 2010; Opdyke et al., 2014; Papadaki et al., 2017; World Meteorological Organization, 2019).

Regardless of the selected method, estimation procedures should take into account the natural variability of river flow driven by the dynamics of climate, catchment land use and domestic, agricultural and industrial consumptions and then of the EF itself. With reference to hydrological methods, a large body of literature was focused on the intra-annual variability for EF assessment, discussing about the different values that EF should be given according to the particular river flow conditions during the year. A monthly based variability was proposed by different authors. The Tessmann method (1980) considers intra-annual variability allocating percentages of monthly flow to calculate EF depending on the different flow seasons (high, intermediate, or low-flow months) (Nyika, 2017). The basic flow methodology (Palau and Alcazar, 2012; Peñas et al., 2014) defines a monthly maintenance flow regime based on the definition of basic and conditioning flows. Gleeson et al. (2012) defined the EF as the monthly flow quantile Q_{90}. In other cases, periods or regimes where different EF values should be considered were recognized. Hanasaki et al. (2008) developed an EF method considering intra-annual variability based on global monthly river flows, defining four different river regimes (dry, wet, stable and variable) and assuming that for each regime EF is represented by a percentage of mean monthly flow. Pastor et al. (2014) proposed a non-parametric method based on flow quantiles, where the annual flow quantile Q90 is allocated during the low flow season and the annual flow quantile Q50 is instead allocated during the high flow period.

Recent approaches also presented the concept that inter-annual variability of flows is furthermore important for the riverine ecosystem. In 1996 Richter et al. (1996) proposed the IHA method based on the identification of Indicators of Hydrologic Alteration, which defines magnitude, timing, frequency, duration and rate of change on natural flow regimes, to define major component of flow that are ecologically important. Since then, a number of applications were presented where, based on the computation of various IHA indices, long term differences in terms of EFs were assessed as a consequence of climate and or anthropogenic changes (Peres and Cancelliere, 2016; Lin et al., 2017; Ren et al., 2018). But the question of the deviation of the EF indices from the natural ranges is far from being fully addressed (Acreman and Dunbar, 2004; Ren et al., 2018). Smakhtin et al. (1997) and Castellarin et al. (2007) proposed an analysis of annual flow duration curves in a regional approach, discussing about how the largest differences between the individual annual curves occur especially during the low flow period of a year but no specific quantification about the inter-annual variability of EFs was attempted so far.

In this framework, the current paper main aims are to:

i) recommend methodologies for EFs and EFs inter-annual variability estimation in a particular climate environment, the Mediterranean basin, where EF assessment is important to quantify the potential water supply for domestic and agricultural consumption under a typical rainfall shortage condition;
ii) test if and, in case, how the recommendation for the most suitable method is influenced by the river basin characteristics, with particular reference to the geological and climate settings, known to be the main drivers of low flow conditions.

With this aims and in the challenge of a regional scale framework for environmental flow and environmental flow variability assessment, where new approaches are generally warmly foreseen (Acreman and Ferguson, 2010; Pastor et al., 2014), a hydrological method, computing EF index from empirical flow duration curve, as a discharge value for a particular duration, was applied to a dataset of 28 non regulated catchments located in southern Italy, covering a region of about 25.000 km^2. The flow size equalling or exceeding 95 % of the time, Q_{95}, was considered as it is a widely used flow index (Olsen et al., 2013; WMO, 2019). In order to describe the Q_{95} inter-annual variability, individual annual flow duration curves (AFDCs) were considered to assess average and standard deviation values for Q_{95} quantiles at each gauged site within the investigated region. One of the most popular method used to predict Q_{95}, the regression approach (Kobold and Brilly, 1994; Castellarin et al., 2007; Laaha and Blöschl, 2007; Mohamoud, 2008; Vezza et al., 2010; Cheng et al., 2012), was applied to predict EF and EF inter-annual variability at the catchment scale (at-site analysis), where morphological and climate descriptors, such as catchment area, precipitation, elevation, land use, geology have been related to the environmental flow indicator. The results of the at-site analysis in terms of average EF and EF statistical variability indices were further analysed over the whole studied area to approach a regional scale tool describing the importance of EFs inter-annual variability. In the end, an approach for its quantitative assessment in a fully regional methodology, where no hydrological observations are available, was suggested.

The findings encourage a feasible identification of systems mostly affected by the EF variability, which would represent an undeniable and interesting finding for future predictions in a global environmental change perspective (Longobardi and Van Loon, 2018).

2. The studied region

The study region is a complex relief area, with inland highlands running north-west to south-east and wide and flat plains facing the Tyrrhenian Sea, where all the river channels included in this analysis flow into. The geology is rather variable: it includes marley-clayey impermeable complex in the north-east area, fissured calcareous and dolomitic complex in the central area, representing the most important regional aquifers with the highest potential infiltration coefficient, and alluvial complex along the coastline. About 30 % of the study area can be considered as permeable and about 32 % is covered by forest.

Hydrologic data consist of daily streamflow time series for 28 non regulated basins mainly located within the Campania region,

Southern Italy, covering a region of about 25.000 km^2 (Fig. 1). The source of streamflow data is the Servizio Idrografico e Mareografico Italiano SIMI. The record length ranges from 6 to 65 years. The size of the basins ranges between 10 and 5000 km^2. The following physiographic and hydrological characteristics were computed for each catchment and indicated in Table 1: drainage area (km^2), mean daily discharge (m^3/s), daily discharge coefficient of variation (%), mean topographic catchment elevation (m), mean topographic catchment slope (%), percentage of forested area (%), and geology, represented by a permeability index PI (%) (Longobardi and Villani, 2013). Additionally the baseflow index BFI (%) was computed by the application of the Lyne and Hollick algorithm for hydrograph separation (Longobardi and Villani, 2008).

The region under investigation is featured by a typical Mediterranean and humid climate, with very marked dry and wet seasons within the year. Mean annual precipitation and air temperature show a moderate gradient form the coastline to the inland. As the investigated catchments are all located along the hill reliefs climate variables are rather homogeneously spatially distributed. The intra-annual precipitation distribution is also homogeneous, with the minimum amount of precipitation observed from June to September and the maximum from November to February (Longobardi and Villani, 2010; Longobardi et al., 2016). Additional climate statistics used for the current analysis, including mean annual precipitation μ(P), annual precipitation coefficient of variation CV(P) (the ratio between the standard deviation and the mean values), mean annual air temperature μ(T), were obtained from the annual time series of precipitation retrieved from an evenly spaced network of 62 thermometric sensors and 163 raingauges distributed over the whole study area (Longobardi and Mautone, 2015). They are illustrated in Table 2.

3. Observing and quantifying EF variability

The FDC is a representation of the cumulative distribution function of streamflow. When recorded streamflow data are available, it can be easily graphically derived, ranking the data and plotting each data for the corresponding plotting position. It is well known that the location and shape of the FCD in the time-discharge domain is dependent on the climate, the geometrical catchment features, and the geology and soil types. In particular for what concerns the study area of interest, in a previous paper it was showed how the shape of the FDC is significantly affected by the proportion of baseflow to total stream flow, the BFI index, with flat and steep FDC shapes associated respectively to high and low BFI indices (Longobardi and Villani, 2013). Similar properties were found in neighbouring region featured by similar hydro-geological characteristics showing the possibility for a generalization of the approach based on the geological properties (Claps and Fiorentino, 1997). Within the study area the BFI index is tightly related to the catchment hydro-geo-morphological properties, summarized by a permeability index PI reported in Table 1 (Longobardi and Villani, 2008). In turn, the FDC shape is mainly affected by the catchment hydro-geo-morphological properties; rainfall properties were showed not to be critical in the FDC shape regional prediction (Longobardi and Villani, 2013).

As discussed in the introduction, Q_{95}, the flow size equalling or exceeding 95 % of the time, was assumed as a measure of EFs in the current study. Empirical Q_{95} assessment requires then necessarily a preliminary construction of the empirical flow duration curve. To assess the EFs average value and inter-annual variability, for each of the gauged stations firstly annual FDCs ("AFDC"), that is FDCs for each single year, were constructed and secondly the empirical average of annual flow duration curves was computed (mean annual

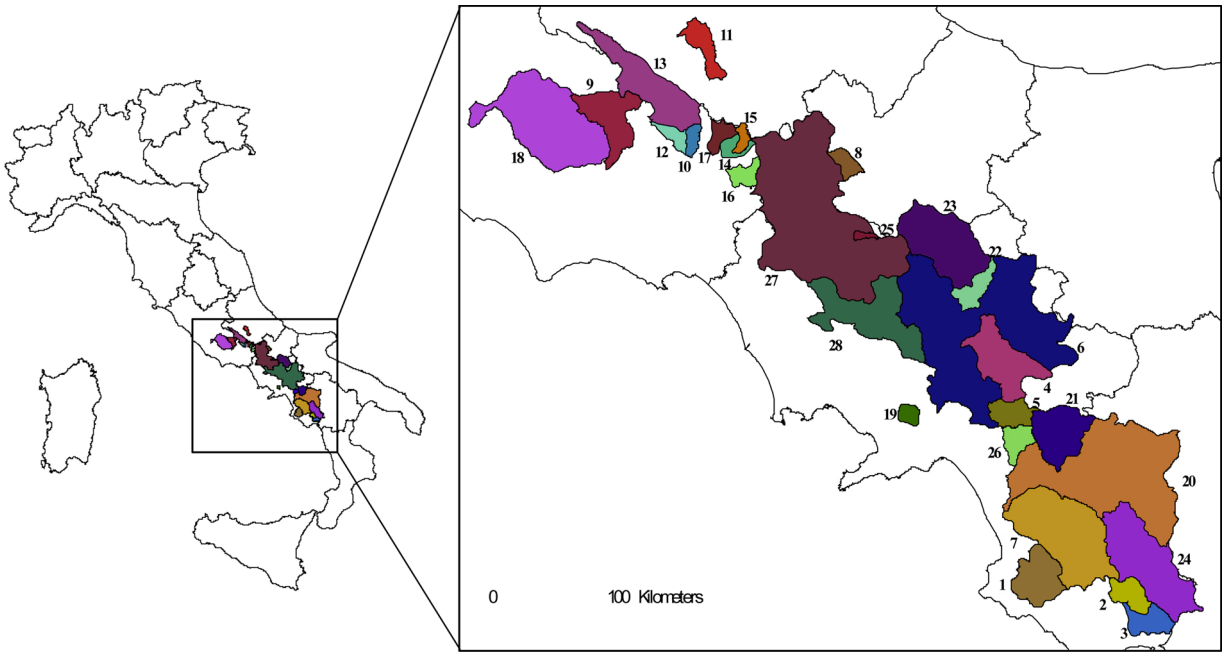

Fig. 1. Catchment locations and map reference numbers as indicated in Table 1.

Table 1
Catchment descriptors used in the study: reference map number, drainage area, mean daily discharge, daily discharge standard deviation, mean topographic catchment elevation, mean topographic catchment slope, percentage of forested area, permeability index and baseflow index.

Catchment	Map ref.	Area (km^2)	μ(Q) (m^3/s)	CV(Q) (%)	h_{mean} (m)	p_{mean} %	FOR %	PI %	BFI %
Alento @ Casalvelino	1	270	4.33	262.82	328	10.4	52	3	32.3
Bussento @ Caselle in Pittari	2	125	5.19	75.72	667	12.7	62	70	70.4
Bussento @ Sicili	3	255	6.48	70.22	779	13.4	65	85	66.2
Calore Irpino @ Apice	4	532	8.64	195.37	611	8.2	30	26	53.8
Calore Irpino @ Montella	5	130	2.11	140.76	1004	13.7	71	84	57.9
Calore Irpino @ Solopaca	6	2991	33.25	199.19	546	7.4	22	13	42.8
Calore Lucano @ Persano	7	805	21.93	226.54	658	10.4	40	14	36.3
Carpino @ Carpinone	8	69	1.71	73.68	898	8.9	55	34	70
Cosa @ Ceccano	9	312	1.61	183.85	728	9.4	36	42	49.9
Fibreno @ Brocco	10	47	9.39	33.65	491	8.3	32	80	87.3
Giovenco @ Pescina	11	138	1	83.00	1298	13.2	26	35	70.4
Liri @ Isola Liri	12	586	28.09	74.62	1024	12.1	52	49	71.2
Liri @ Sora	13	480	14.88	129.91	1060	12.3	57	55	64.1
Melfa @ Atina	14	86	3.96	107.83	1397	21.1	49	97	67.6
Melfa @ Picinisco	15	38	0.91	79.12	1074	15.8	78	68	66.4
Rapido @ S. Elia Fiumerapido	16	73	1.75	33.71	816	12.4	60	87	83.9
Rio Mollo @ Settignano	17	69	0.71	377.46	946	13	26	10	25.3
Sacco @ Ceccano	18	912	11.21	275.74	439	7.3	25	10	33.7
Sarno @ S. Valentino Torio	19	46	8.64	28.94	240	9.8	11	70	85.9
Sele @ Albanella	20	3216	55.61	159.81	684	10	39	36	54.3
Sele @ Contursi	21	322	10.12	162.15	711	12.4	46	47	58.3
Tammaro @ Paduli	22	675	9.26	161.56	597	6.1	17	8	42.1
Tammaro @ Pago Veiano	23	558	6.02	186.71	633	6.1	20	10	39.4
Tanagro @ Polla	24	660	9.72	155.35	792	9.4	39	48	48
Torano@ Piedimonte Matese	25	18	3	43.00	949	15.1	78	85	85.2
Tusciano @ Olevano sul Tusciano	26	102	3.6	72.22	961	15.8	85	78	73.3
Volturno @ Amorosi	27	2029	36.69	152.74	590	9.4	45	39	54.7
Volturno @ Cancello Arnone	28	5586	80.45	137.76	534	8.2	31	26	55.2

Table 2
EF and rainfall measures used in the study: Q95 quantile average μ(Q95) and coefficient of variation CV(Q95), mean annual precipitation μ(P), annual precipitation coefficient of variation CV(P) and mean annual air temperature μ(T).

Catchment	$\mu(Q_{95})$ (m3/s)	$CV(Q_{95})$ %	μ(P) (mm)	CV(P) %	μ(T) °C
Alento @ Casalvelino	0.31	87.10	1254	22.00	15.21
Bussento @ Caselle in Pittari	2.27	20.70	1398	23.63	12.83
Bussento @ Sicili	3.58	11.73	1589	23.10	12.05
Calore Irpino @ Apice	2.78	60.07	1119	21.18	13.23
Calore Irpino @ Montella	0.38	81.58	1417	21.89	10.47
Calore Irpino @ Solopaca	4.5	68.67	1107	20.37	13.68
Calore Lucano @ Persano	3.68	50.00	1362	24.09	12.90
Carpino @ Carpinone	0.72	51.39	1077	20.84	11.22
Cosa @ Ceccano	0.21	85.71	1417	21.17	12.41
Fibreno @ Brocco	7.2	25.69	1369	19.52	14.07
Giovenco @ Pescina	0.66	22.73	859	20.42	8.41
Liri @ Isola Liri	15.23	23.70	1251	24.00	10.33
Liri @ Sora	7.02	41.45	1107	24.86	10.08
Melfa @ Atina	1.1	71.82	1572	19.37	7.72
Melfa @ Picinisco	0.33	60.61	1492	19.35	9.98
Rapido @ S. Elia Fiumerapido	1.36	19.12	1463	19.78	11.79
Rio Mollo @ Settignano	0.03	86.67	1378	19.24	10.88
Sacco @ Ceccano	1.28	49.22	1268	22.45	14.43
Sarno @ S. Valentino Torio	6.6	27.88	1032	21.61	15.83
Sele @ Albanella	15.83	67.91	1197	22.83	12.72
Sele @ Contursi	4.99	22.44	1336	22.38	12.53
Tammaro @ Paduli	0.13	115.38	992	19.60	13.33
Tammaro @ Pago Veiano	0.21	138.10	1102	19.82	13.07
Tanagro @ Polla	2.13	35.68	1288	24.46	11.96
Torano@ Piedimonte Matese	2.22	32.43	1283	22.47	10.86
Tusciano @ Olevano sul Tusciano	1.74	15.52	1633	22.16	10.77
Volturno @ Amorosi	12.74	54.24	1387	20.84	13.37
Volturno @ Cancello Arnone	26.47	41.25	1183	20.59	13.77

FDC). As an example Fig. 2 illustrates the ADFCs and mean annual FDC at four of the considered streamflow gauged sites. It is evident, as previously mentioned in the description of the general features of the investigated region, how small PI indices are associated to steeper FDCs. Small PI indices also seem to be related to wider AFDCs envelope. The results of the regional scale analysis will better describe this particular characteristic in the next paragraphs.

For each AFDCs, the 95 % probability of exceedance was considered and Q_{95} discharge was computed (Fig. 3). The average and the coefficient of variation (the ratio between the standard deviation and the mean values) of Q_{95} for each catchment, $\mu(Q_{95})$ and $CV(Q_{95})$, are reported in Table 2. The region under investigation appears quite heterogeneous with $\mu(Q_{95})$ ranging between 0.03 mc/s to 25.46 mc/s (referred to the largest drainage catchment in the region of about more than 5000 km^2). The Q_{95} variability is also markedly heterogeneous with $CV(Q_{95})$ ranging 11 %–138 %.

To quantify the inter-annual Q_{95} variability for the specific case study, the confidence boundaries for $\mu(Q_{95})$ were reconstructed for different significance levels and indicated as $Q_{95inf,\alpha}$ and $Q_{95sup,\alpha}$ ($\alpha = 0.99$, 0.95 and 0.9). For each catchment, the maximum and minimum Q_{95} values, Q_{95max} e Q_{95min}, were quantified as the Q_{95} corresponding to the upper boundary and lower boundary curves of the AFDCs envelopment. The corresponding values were compared with the confidence boundaries values $Q_{95sup,\alpha}$ and $Q_{95inf,\alpha}$. Table 3 reports, for the different significance levels, the percentage of catchments for which Q_{95min} or Q_{95max} are outside the confidences boundaries, that is for which $Q_{95min} < Q_{95inf,\alpha}$ and $Q_{95max} > Q_{95sup,\alpha}$. It can be observed that, for example with reference to $\alpha = 0.95$, the zero hypothesis ($Q_{95} = \mu(Q_{95})$) was rejected in the 32 % of the cases, that is the observed Q_{95min} is significantly different from $\mu(Q_{95})$ for 32 % of gauged stations. Even more markedly, Q_{95max} is significantly different from the $\mu(Q_{95})$ for 75 % of gauged stations.

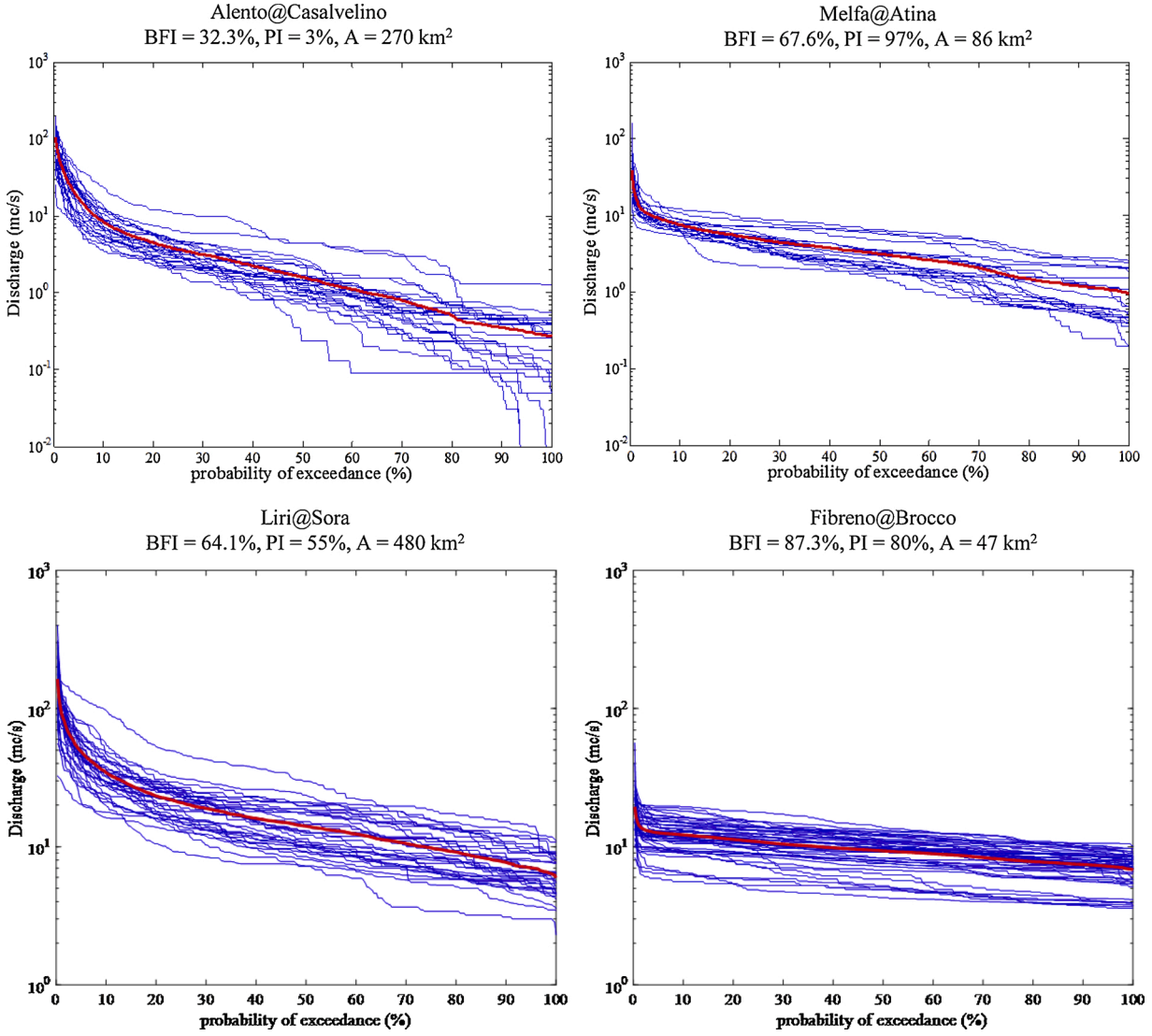

Fig. 2. AFDCs (blue thin lines) and mean annual FDC (red thick line) at four gauged sites within the study region. Displayed catchments permeability indices PI cover the range of variability of the investigated area.

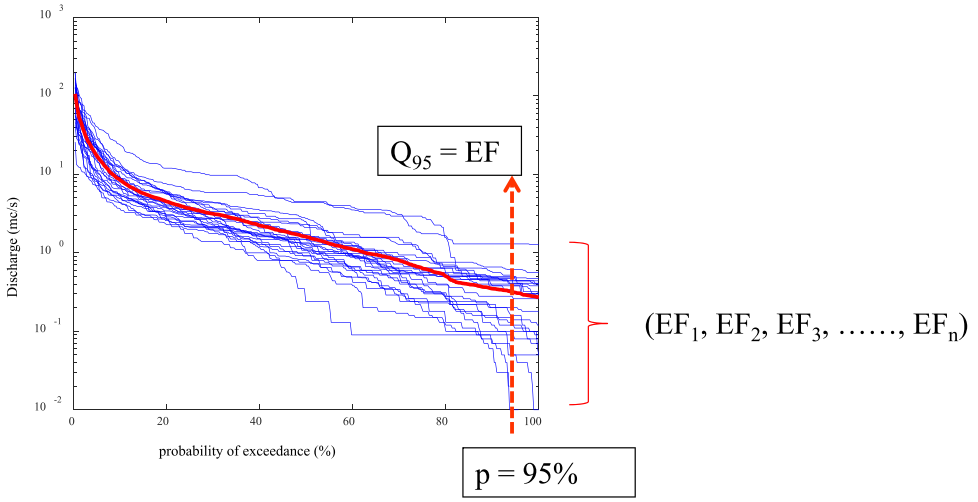

Fig. 3. An example of AFDCs envelope and EFs inter-annual variability assessment.

Table 3
Percentage of catchments for which Q95 min < Q95 in.,α (lower envelopment) and Q95max > Q95sup,α (upper envelopment).

Significance level (%)	$Q_{95min} < Q_{95inf,\alpha}$ (lower envelopment curve)	$Q_{95max} > Q_{95sup,\alpha}$ (upper envelopment curve)
1	0	25
5	32	75
10	36	82

Table 4
Q95 regression prediction model performances and jackknife errors estimates (MOD1).

Catchments	μ (mc/s)	CV (%)	rmse (mc/s)	r^2cor (-)	mt (-)	ma (-)	me (-)
Alento @ Casalvelino	0.32	53.86	0.05	0.38	0.93	0.85	0.09
Bussento @ Caselle in Pittari	2.30	11.86	0.12	0.13	0.17	0.14	0.03
Bussento @ Sicili	3.55	5.60	0.02	0.51	0.10	0.08	0.03
Calore Irpino @ Apice	2.84	27.68	1.90	0.27	0.76	0.72	0.04
Calore Irpino @ Montella	0.40	47.99	0.06	0.35	1.20	1.15	0.05
Calore Irpino @ Solopaca	4.47	59.45	2.69	0.66	0.41	0.35	0.06
Calore Lucano @ Persano	3.90	4.04	2.72	−0.03	0.42	0.40	0.03
Carpino @ Carpinone	0.68	32.67	0.08	0.34	0.60	0.41	0.19
Cosa @ Ceccano	0.21	61.23	0.02	0.39	1.10	0.97	0.13
Fibreno @ Brocco	7.21	4.95	3.26	0.01	0.25	0.24	0.01
Giovenco @ Pescina	0.66	3.18	0.03	−0.05	0.19	0.17	0.02
Liri @ Isola Liri	15.21	8.56	12.86	0.05	0.23	0.21	0.02
Liri @ Sora	7.24	14.83	6.35	0.12	0.32	0.29	0.02
Melfa @ Atina	1.09	33.18	0.47	0.23	0.81	0.74	0.07
Melfa @ Picinisco	0.34	29.63	0.04	0.15	0.47	0.40	0.07
Rapido @ S. Elia Fiumerapido	1.37	4.29	0.07	−0.05	0.18	0.16	0.02
Rio Mollo @ Settignano	0.04	55.59	0.00	0.69	1.00	0.62	0.38
Sacco @ Ceccano	1.30	11.91	0.40	−0.03	0.46	0.41	0.06
Sarno @ S. Valentino Torio	6.56	13.32	2.64	0.14	0.24	0.22	0.02
Sele @ Albanella	16.14	32.83	89.92	0.22	0.55	0.51	0.04
Sele @ Contursi	5.01	1.86	1.28	−0.02	0.22	0.21	0.01
Tammaro @ Paduli	0.15	24.85	0.03	−0.04	2.71	2.38	0.33
Tammaro @ Pago Veiano	0.30	33.27	0.09	0.05	4.53	3.92	0.61
Tanagro @ Polla	2.14	10.81	0.53	0.09	0.34	0.32	0.01
Torano@ Piedimonte Matese	2.22	4.99	0.56	−0.02	0.27	0.25	0.02
Tusciano @ Olevano sul Tusciano	1.76	3.39	0.09	−0.09	0.15	0.13	0.03
Volturno @ Amorosi	12.72	35.19	23.78	0.48	0.58	0.56	0.03
Volturno @ Cancello Arnone	26.49	20.47	82.76	0.27	0.38	0.36	0.02
regional averages			8.32	0.19	0.70	0.61	0.09

It is clear how, at least for the studied region, including an assessment of EF inter-annual variability would represent a valuable added value for regional scale assessment tools.

4. EF and EF inter-annual variability: at site-analysis

A database regression analysis framework was applied to explain the year to year Q_{95} variability at each gauged site (inter-annual variability). A time series of Q_{95} was reconstructed selecting the Q_{95} discharge from the single AFDCs and it was regressed against related time series of annual precipitation P, mean annual daily discharge Q and annual BFI index. The last was derived in a year by year hydrograph separation of total discharge by the use of the Lyne and Hollick algorithm (Longobardi and Villani, 2008). The BFI index and the discharge Q were demonstrated to be the most significant descriptors to be used for low flow prediction within the geographical region the investigated catchments belong to (Longobardi and Villani, 2008).

In particular the three following regression models were calibrated over each gauged site:

$$\text{MOD 1: } Q_{95} = a_1 + a_2 * \text{BFI} \tag{1}$$

$$\text{MOD 2: } Q_{95} = b_1 + b_2 * \text{BFI} + b_3 * Q \tag{2}$$

$$\text{MOD 3: } Q_{95} = c_1 + c_2 * \text{BFI} + c_3 * Q + c_4 * P \tag{3}$$

Models were compared in terms of conventional statistics, such as the mean, standard deviation (std), coefficient of variation (CV), the root mean squared error (rmse) and the Pearson correlation coefficient (r^2cor), corrected for the number of model parameters:

$$r^2_{cor} = 1 - (1 - r^2)\frac{k-1}{k-p} \tag{4}$$

where p is the number of model parameters and k is the sample length. Results are given in Tables 4 and 5 for what concerns Eqs. (1) and (2), respectively. The same tables also provide the cross-validation errors estimates derived from the application of the jackknife resampling procedure, to assess different sources of error (Efron, 1982):

- mean total true error "mt", the average error over the whole sites, for each of which the prediction is made with the parameters obtained by excluding from the dataset the observation referring to the site for which the prediction is computed (leave-one-out validation);

Table 5
Q95 regression prediction model performances and jackknife errors estimates (MOD2).

Catchments	μ (mc/s)	CV (%)	rmse (mc/s)	r^2cor (-)	mt (-)	ma (-)	me (-)
Alento @ Casalvelino	0.31	62.66	0.02	0.73	1.02	0.90	0.13
Bussento @ Caselle in Pittari	2.31	14.76	0.12	0.16	0.16	0.12	0.04
Bussento @ Sicili	3.72	7.30	0.03	0.27	0.12	0.04	0.07
Calore Irpino @ Apice	2.85	45.26	0.98	0.62	0.40	0.36	0.04
Calore Irpino @ Montella	0.40	50.21	0.06	0.39	1.24	1.17	0.07
Calore Irpino @ Solopaca	4.44	62.88	2.17	0.73	0.35	0.27	0.09
Calore Lucano @ Persano	3.91	23.40	2.14	0.19	0.34	0.31	0.03
Carpino @ Carpinone	0.64	44.97	0.09	0.24	0.50	0.29	0.21
Cosa @ Ceccano	0.22	67.08	0.02	0.43	1.03	0.81	0.22
Fibreno @ Brocco	7.21	24.13	0.48	0.85	0.08	0.08	0.01
Giovenco @ Pescina	0.66	20.78	0.01	0.81	0.10	0.08	0.02
Liri @ Isola Liri	15.41	23.64	3.56	0.74	0.12	0.10	0.02
Liri @ Sora	7.28	32.91	2.63	0.64	0.22	0.19	0.03
Melfa @ Atina	1.11	61.33	0.16	0.74	0.41	0.36	0.05
Melfa @ Picinisco	0.32	45.80	0.01	0.78	0.32	0.25	0.06
Rapido @ S. Elia Fiumerapido	1.36	18.15	0.01	0.82	0.06	0.05	0.01
Rio Mollo @ Settignano	0.06	66.21	0.00	0.94	2.54	0.53	2.01
Sacco @ Ceccano	1.38	37.06	0.41	−0.06	0.55	0.39	0.17
Sarno @ S. Valentino Torio	6.57	26.16	0.65	0.79	0.13	0.10	0.02
Sele @ Albanella	16.19	45.02	63.20	0.45	0.49	0.44	0.05
Sele @ Contursi	5.03	10.56	1.10	0.12	0.20	0.18	0.02
Tammaro @ Paduli	0.15	74.76	0.02	0.44	1.76	1.49	0.26
Tammaro @ Pago Veiano	0.28	46.76	0.10	0.00	4.38	3.64	0.74
Tanagro @ Polla	2.14	28.05	0.23	0.60	0.19	0.18	0.01
Torano@ Piedimonte Matese	2.21	30.74	0.07	0.87	0.11	0.10	0.01
Tusciano @ Olevano sul Tusciano	1.75	12.34	0.03	0.62	0.09	0.07	0.02
Volturno @ Amorosi	12.72	51.12	5.63	0.88	0.19	0.17	0.02
Volturno @ Cancello Arnone	26.46	31.99	53.79	0.52	0.26	0.24	0.02
regional averages			4.92	0.55	0.62	0.46	0.16

- mean apparent error "ma", the average error over the whole sites, for each of which the prediction is made with the parameters obtained by the whole dataset of observations;
- mean expected excess error "me", the difference between the mean total true error and the mean apparent error.

The mean apparent error measures the goodness of the adaptation of the regional relationship to the whole dataset (descriptive abilities) whereas the mean expected excess error measures its reliability in terms of robustness (predictive abilities).

For sake of conciseness, the results which refer to the calibration of MOD3 were not here reported as the main statistic and performance errors are substantially coincident with the results associated to MOD2, showing the relative poor capability of the total annual rainfall to further contribute to the description of the EF average values likely because already embedded within the Q variability accounted for in MOD1 and MOD2.

At the regional scale, the MOD2 regression model, including the BFI index and the mean annual discharge as independent variables, appeared to be the best performing model (Tables 4 and 5). In particular Q appeared to be the most significant independent variable: the average (over the region) explained variance of MOD1 is about 19 % (max $r^2_{corr} = 0.51$ and min $r^2_{corr} = -0.09$) and it increased up to 55 % in the case of MOD2 (max $r^2_{corr} = 0.94$ and min $r^2_{corr} = -0.06$).

Predicted average values for Q_{95} were almost equal to the observed ones for both MOD1 and MOD2 (Fig. 4 left panels). MOD1 underestimated the Q_{95} coefficient of variation of about 47 % (Fig. 4 right upper panel) whereas MOD2 generated an average underestimation of about 37 %. Prediction of large CV was particularly uncertain, but in the case of MOD2, likely the existence of the independent variable Q in the regression model, generated more robust estimates.

Differences between regression models were also detected for what concerns the jackknife error statistic, with an important increase of mean expected excess error (me), a measure of model robustness, from 9% in the case of MOD1 to 16 % in the case of MOD2.

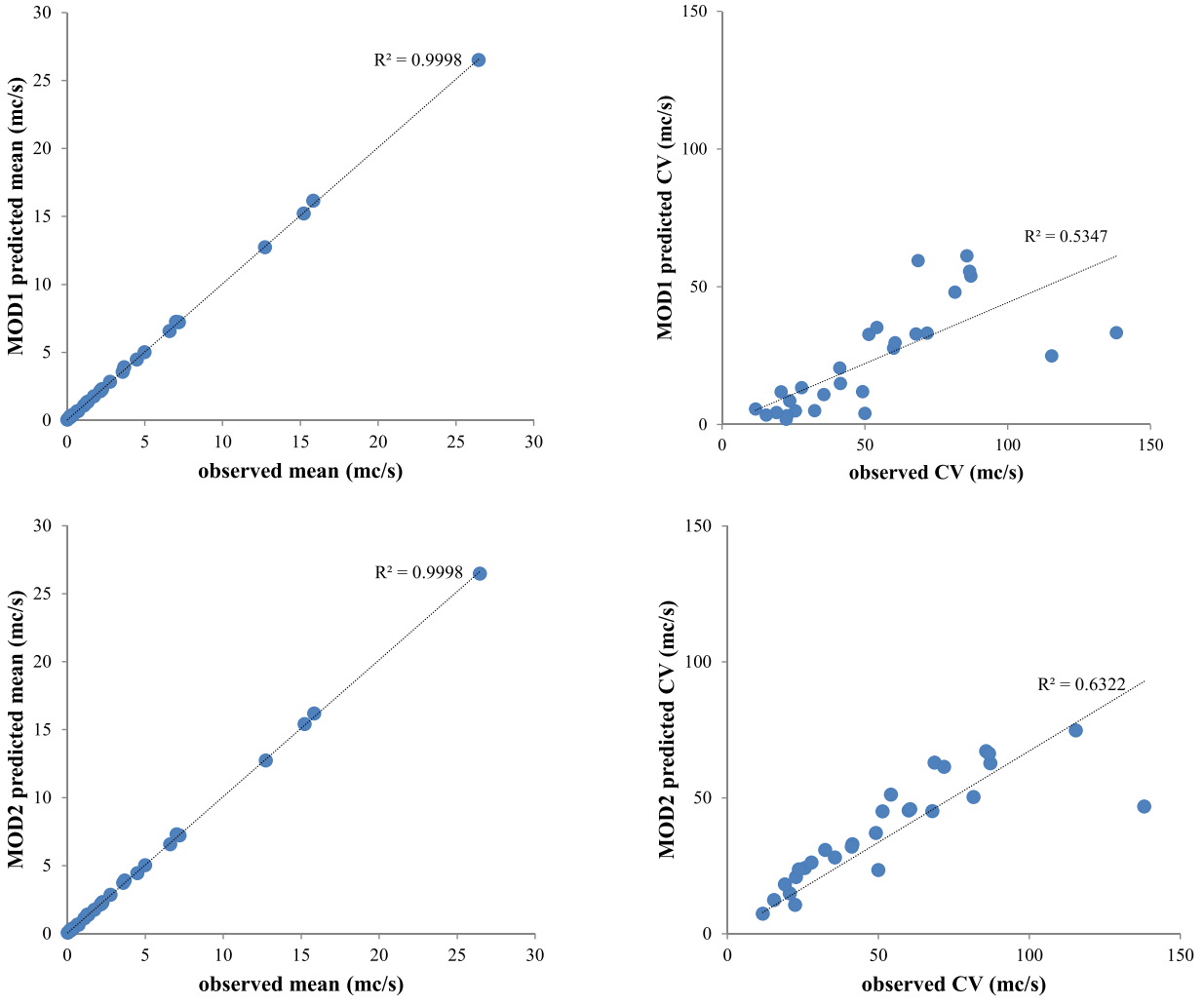

Fig. 4. Comparison between observed and predicted Q95 mean and coefficient of variation for MOD1 (upper panel) and MOD2 (lower panel). The line represents the bisector of the observed-predicted plot area.

As an example, Fig. 5 illustrates EF, Q and BFI time series for two very different catchments. Fig. 5 left panel shows the case of a medium range PI catchment, the Liri@Sora, with an average BFI equal to 64 % whereas Fig. 5 right panel shows the case of a high PI catchment, the Fibreno@Brocco, with an average BFI equal to 87 % (Table 1). The Fibreno catchment has lower discharge and EF values mainly due to the smaller drainage area compared to the Liri catchment. The large and mainly constant BFI values indicate a system where streamflow is strongly sustained by the groundwater contribution. As a consequence, its FDC (as illustrated in Fig. 2 lower right panel), would be flat, Q and EF have very strongly correlated patterns, almost similar magnitude and a very moderate variability in time (Fig. 5 right panel). In the case of the Liri catchment (Fig. 5 left panel), Q and EF have still well correlated patterns, even though EF has a smaller variability and a significantly smaller magnitude compared to Q. The BFI values are quite variables and the EF pattern variability in the case of the Liri catchment is also more marked compared to the Fibreno catchment. This is also seen in the comparison of the empirical CV(Q) indices, respectively 130 % and 33 % (Table 1) and of the empirical CV(Q_{95}) indices, respectively 41 % and 25 % (Table 2). For what concerns the climate feature, the Liri catchment is furthermore featured by a large CV (P), of about 24 %, compared to the Fibreno catchment, which CV(P) amounts to about 19 % (Table 2).

5. EF and EF inter-annual variability: regional analysis

The at-site analyses highlighted the importance of the mean annual daily discharge Q and the BFI index in the prediction of Q_{95} and its variability. They furthermore showed how apparently the annual precipitation is not able to additionally, beyond Q and BFI, explain the average Q_{95} and its variability. Drainage area seemed to matter but, clearly, its role was not be explicitly accounted for into the at-site investigation.

The regional scale analysis aimed to calibrate regional empirical relationships to predict the average Q_{95} and its variability, summarized by the CV, starting from synthetic catchment descriptors, widely and readily available at the regional scale. In particular indices reported in Tables 1 and 2 were accounted for the purpose. A matrix of correlation coefficients (if only larger than 10 %) is reported in Table 6, as a starting point to identify the dominant variables and to define the empirical regional laws. The average Q_{95} appeared to be mainly related to basically drainage area A and average daily discharge μ(Q). BFI was poorly related to μ(Q_{95}) but due to its conceptual value, its role in the definition of the regional laws was explored. CV(Q_{95}) appeared instead correlated to different indices, included the precipitation index CV(P). Correlation coefficients appeared however rather weak, with the most correlated index being the BFI ($r^2 = 0.46$).

5.1. Mean Q_{95} assessment

Starting from the results illustrated in Table 6, a step-wise regression approach indicated the mean daily streamflow μ(Q) to be the dominant variable for μ(Q_{95}) prediction at the regional scale. It explained indeed up to 84 % of the variance (Fig. 6 left panel).

The explained variance increased up to 92 % when also catchment drainage area A is accounted for and in the end a very moderate increase, up to 95 %, is provided when in the regression model the BFI index is furthermore considered. The relevant equations for regional μ(Q_{95}) index are reported in Table 7.

To assess and compare models performance, the Average Percentage Error APE index was computed as:

$$APE = \frac{1}{n}\sum_{i=1}^{n}\frac{\mu(Q_{95})_{obs} - \mu(Q_{95})_{pred}}{\mu(Q_{95})_{obs}} \quad (5)$$

where $\mu(Q_{95})_{obs}$ and $\mu(Q_{95})_{pred}$ are respectively the observed and regional predicted Q_{95} average values and n is the number gauged sites. The APE index assessment for each gauged station, referred to the catchment BFI index, is illustrated in Fig. 7. If catchment area was also accounted for, the APE index was strongly smaller compared to the case when only μ(Q) was considered (single regression model in Fig. 7), but then it increases again when the BFI was additionally included in the regression, even though the multiple regression model using three independent variables represented the best performing according to the correlation coefficient (Table 7). The increase in the APE index when the three independent variables (μ(Q), A, BFI) were considered, was mainly due to the prediction

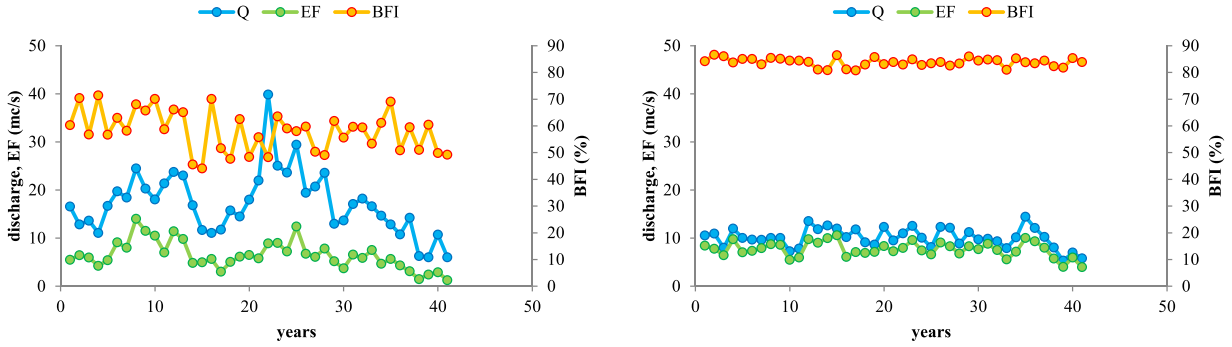

Fig. 5. Annual time series of EF, Q and BFI for the Liri@Sora (A = 480 km2; left panel) and Fibreno@Brocco (A = 47 km2; right panel).

Table 6
Pearson correlation coefficients for the catchment attribute indices considered in the current study. Only correlation coefficients larger than 10 % were reported.

	$\mu(Q_{95})$	$CV(Q_{95})$	A	$\mu(Q)$	CV(Q)	PI	h_{mean}	p_{mean}	FOR	BFI	μ (P)	CV(P)
$\mu(Q_{95})$	1											
$CV(Q_{95})$	–	1										
A	0.63	–	1									
$\mu(Q)$	0.84	–	0.91	1								
CV(Q)	–	0.33	–	–	1							
PI	–	0.29	0.13	–	0.58	1						
h_{mean}	–	–	–	–	–	0.18	1					
p_{mean}	–	0.11	0.15	0.10	–	0.47	0.56	1				
FOR	–	0.14	–	–	0.17	0.39	0.22	0.45	1			
BFI	–	0.46	–	–	0.89	0.67	–	0.16	0.17	1		
μ(P)	–	–	–	–	–	0.31	–	0.34	0.40	–	1	–
CV(P)	–	0.17	–	–	–	–	–	–	–	–	–	1

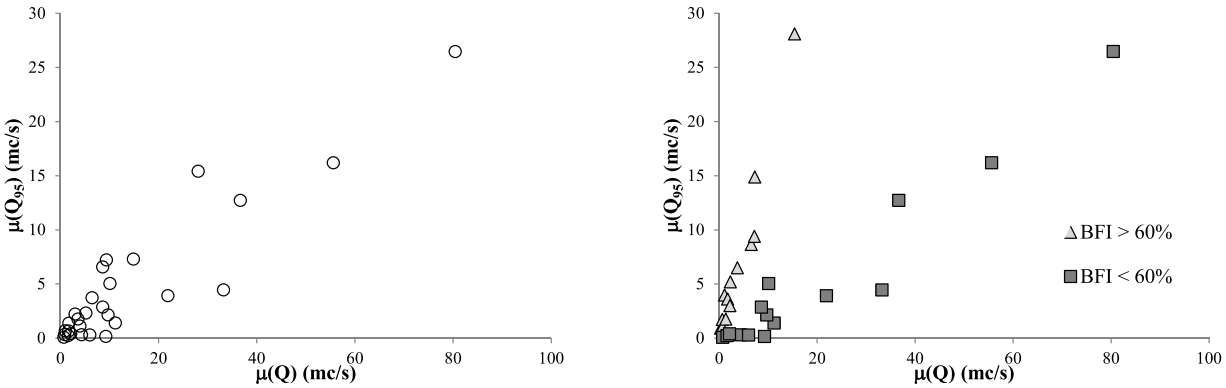

Fig. 6. μ(Q95) dependence on μ(Q): for the whole region (left panel) and for BFI classes within the region (right panel).

Table 7
μ(Q95) single and multiple regression models for the investigated region.

Regression model	r^2_{corr}	APE(%)	Valid for
$\mu(Q_{95}) = +0.298 + 0.308*\mu(Q)$	0.84	−211.03	Whole region
$\mu(Q_{95}) = -0.294 + 0.004*A + 0.606*\mu(Q)$	0.92	−30.26	Whole region
$\mu(Q_{95}) = -4.11 + 0.003*A + 0.537*\mu(Q) + 0.065*BFI$	0.95	268.62	Whole region
$\mu(Q_{95}) = \begin{cases} -1.118 + 0.320 * \mu(Q) \\ +0.111 + 0.554 * \mu(Q) \end{cases}$	0.96	16.35	Whole region, with BFI < 60 % Whole region, with BFI > 60 %

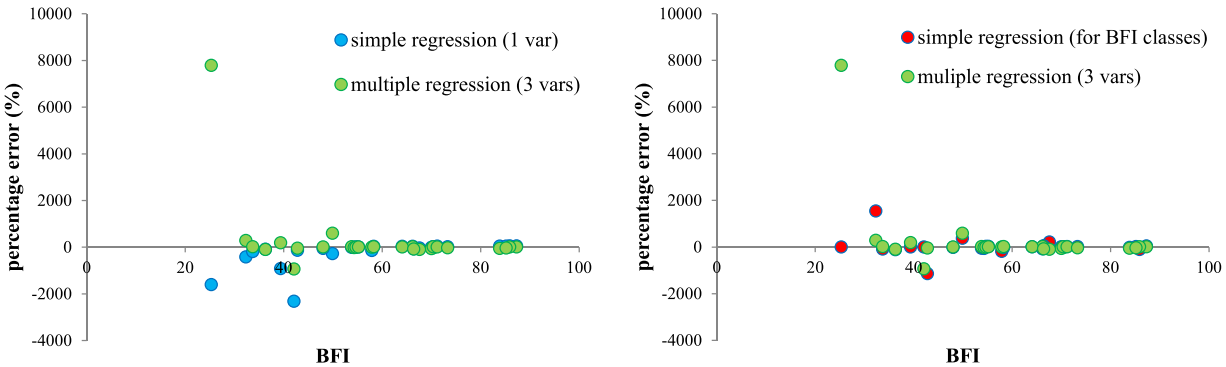

Fig. 7. μ(Q95) regression models percentage prediction errors. In the left panel the single and multiple regression (3 independent variables) models, calibrated over the whole region are compared. In the right panel, the performance of the simple regression model, calibrated for classes of BFI, is compared to the performance of the multiple regression model (3 independent variables).

error associated to a particular catchment (APE index of about 8000 %), as illustrated in Fig. 7 (left panel). The Riomollo@Settignano falls within the class of the watershed featured by small drainage area and low permeability index, which represents indeed the class for which the predictions are rather uncertain in the investigated region. If this was removed from the computation of the APE, the index would decrease up to - 9.82 %.

The prediction errors associated to the simple linear regression model (when only $\mu(Q)$ is considered) appeared important especially for catchments featured by low BFI values (Fig. 7 left panel). The simple regression model prediction capabilities can be indeed improved if the calibration of the regression parameters was performed for groups of catchments identified on the base of the BFI index values (Longobardi and Van Loon, 2018). A threshold value of BFI = 60 % was found for the case study as the value that optimize the single regression models calibration. The BFI threshold identified two groups, a poorly-drained group of catchments, with low groundwater contribution and BFI < 60 % and a well-drained group of catchment, with large groundwater contribution and BFI > 60 %. The calibrated parameters and model equations to be applied for the two groups are reported in Table 7, along with the model performances. Percentage errors, in comparison with the multiple regression model, are illustrated in Fig. 7 right panel. The identification of groups of catchments on the base of the BFI helped to objectively overcome the biased overestimation of the average Q_{95} in the case of the poorly-drained watersheds (where the Riomollo@Settignano is included), as also demonstrated by the correlation coefficients and the APE index improvements illustrated in Table 7.

To further illustrate the importance of the catchment drainage area in the regional assessment of $\mu(Q_{95})$, the same regional models reported in Table 7, were calibrated using the specific mean annual discharge, $\mu_S(Q)$, and the specific mean Q_{95}, $\mu_S(Q_{95})$, that is the $\mu(Q)$ and $\mu(Q_{95})$ values divided by the catchment drainage area. Results are illustrated in Table 8.

Even though the correlation coefficient between observed and modelled $\mu_S(Q_{95})$ appear larger than in the case of $\mu(Q_{95})$, APE errors appear extremely larger and mainly due to very important errors associated to the catchments characterized by the smaller drainage area values and low permeability index (such as in the case of the Riomollo@Settignano). For this specific reason, in the following regional prediction models for $\mu(Q_{95})$ in Table 7 were taken into account.

5.2. Q_{95} inter-annual variability assessment

At the regional scale, $CV(Q_{95})$ was assumed as a measure for Q_{95} inter-annual variability. Similarly to what considered in the case of the regional analysis for $\mu(Q_{95})$, a step wise regression highlighted the dominant regional variables for $CV(Q_{95})$ among the catchment indices, as reported in Table 6.

For what concerns the variability of $CV(Q_{95})$ at the regional scale, contrarily from what found in the case of $\mu(Q_{95})$ regression analysis, the drainage area A and the mean annual discharge $\mu(Q)$ did not play a central role. This was probably due to the fact that the coefficient of variation represents a normalized index which is generally adopted in statistical hydrology analyses in order to compare variables whose average values are rather different.

Even though the correlation coefficient indicates a moderate correlation ($r^2 = 0.46$), the BFI appeared as the catchment index that best represent the $CV(Q_{95})$ variability at the regional scale, with large $CV(Q_{95})$ associated to low BFI values (Fig. 8 left panel). This feature highlighted how groundwater poorly sustained catchments correspond to the systems which are more impacted by the environmental flow variability.

A simple regression model that sees the BFI index as the independent variable was the basic model to describe the Q_{95} variability for the studied area. The second best correlated independent variable to $CV(Q_{95})$ was the climate index related to the rainfall variability, that is the CV(P). Including the CV(P) in a regional regression model beyond BFI, increased the explained variance up to 61 % and reduced the APE index from about -24 % to -17 %. The examined regression equations, including model performances, are reported in Table 9.

The average percentage errors for the simple and multiple regression prediction models are illustrated as function BFI and CV(P) respectively in Fig. 9 left and right panel. Both the simple and multiple regression equations predicted an overestimation in $CV(Q_{95})$ assessment. Magnitude errors seemed larger for large BFI values and large CV(P) values.

Similarly to the case of the $\mu(Q_{95})$ prediction, the investigated catchments were subdivided into two groups. The CV(P) was used in this case to identify the groups with respect to the regional average CV(P), which amount to about 21 %. A group of catchments featured by large rainfall variability, with CV(P) >21 % and a group of catchments featured by low rainfall variability, with CV(P) <21 %, were identified.

Taking into account the grouping resulted in a very moderate increase in the explained variance but in a more marked reduction in the APE index, reducing the large $CV(Q_{95})$ overestimation for all of the studied catchments. Although the predictive capabilities of the model were significantly improved, the identification of the groups helped to better specify which systems are most affected by the EF variability and to quantify their variabilities. The patterns identified in Fig. 8 right panel in fact showed how, compared with catchments featured by CV(P) below the regional value, for catchments featured by CV(P) above the regional value, small variations in the BFI correspond to important variations of the $CV(Q_{95})$. Therefore, the level of inter-annual precipitation variability appeared important in the assessment of EF variability only for watershed featured by small BFI values, whereas the rainfall inter-annual variability did not affect the EF variability in the case of catchments characterized by large BFI values.

6. Implication for a fully regional model for $\mu(Q_{95})$ and $CV(Q_{95})$ prediction

In the previous paragraphs regional relationship for the prediction of $\mu(Q_{95})$ and $CV(Q_{95})$ were calibrated. The best performing prediction equations were based on hydrological variables and physical catchment attributes. In particular the mean annual daily

Table 8
Specific μS(Q95) single and multiple regression models for the investigated region.

Regression model	r^2_{corr}	APE(%)	Valid for
$\mu s(Q_{95}) = -0.0092 + 0.794*\mu s(Q)$	0.98	−518.26	Whole region
$\mu s(Q_{95}) = -0.0013 + 4.03*10^{-7}*A + 0.80*\mu s(Q)$	0.92	−520.02	Whole region
$\mu s(Q_{95}) = -5.18 + 0.0044*A + 15.60*\mu s(Q) + 0.097*BFI$	0.95	−11936	Whole region

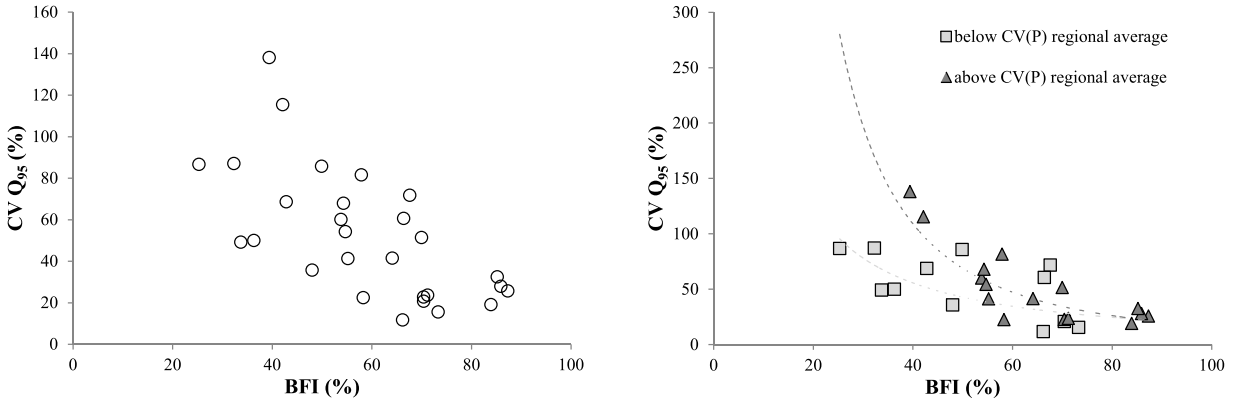

Fig. 8. CV(Q95) dependence on BFI: for the whole region (left panel) and for CV(P) classes within the region (right panel).

Table 9
CV(Q95) single and multiple regression models for the investigated region.

Regression model	r^2_{corr}	APE(%)	Valid for
$CV(Q_{95}) = 0.2086*BFI^{-1.28}$	0.46	−24.37	Whole region
$CV(Q_{95}) = 2.909 - 1.202*BFI - 0.077*CV(P)$	0.61	−17.23	Whole region
$CV(Q_{95}) = \begin{cases} +0.1896 * BFI^{-1.176} \\ +0.1653 * BFI^{-2.059} \end{cases}$	0.63	−9.73	Whole region, with CV(P)< 21 % Whole region, with CV(P) > 21 %

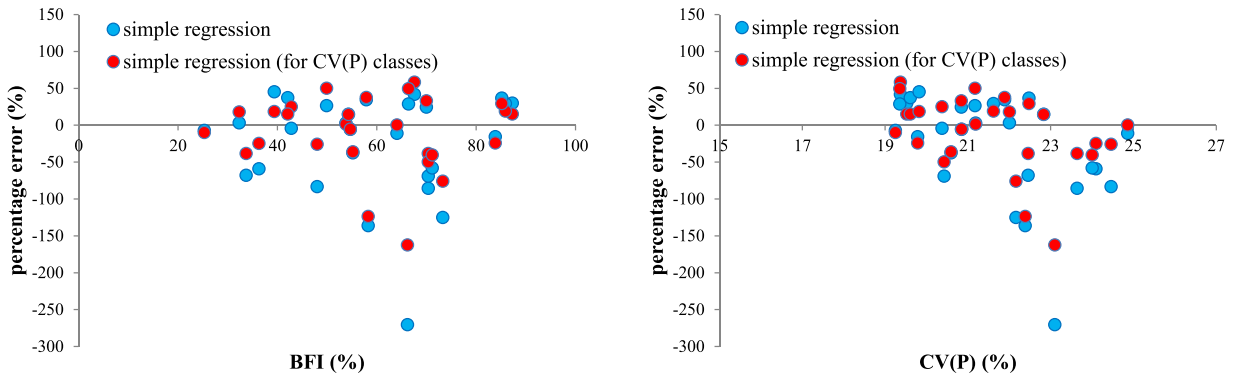

Fig. 9. CV(Q95) regression models percentage prediction errors. In the left panel the single and multiple regression (2 independent variables) models, are plotted against BFI. In the right panel the single and multiple regression (2 independent variables) models, are plotted against CV(Q95).

discharge μ(Q), the BFI, the coefficient of variation of the precipitation CV(P) and the catchment area A appeared the dominant characteristics at the regional scale.

Starting from the summarized findings, an implication for a fully regional approach was proposed for applications in fully ungauged catchments. The fully regional model was intended to simply rely on physical catchment attributes, also embedding the impact of hydrological variables which necessarily originate from continuous observations, unavailable for ungauged sites.

For what concerns the mean annual daily discharge, μ(Q), a first assessment at the regional scale, $\mu(Q)_A$, was provided by the relationship with the catchment drainage area A:

$$\mu(Q)_A = 0.014 \cdot A + 3.02 \quad (6)$$

A strong linear correlation between μ(Q) and A, of about 91 % is reported in Table 6. Fig. 10 left panel compares $\mu(Q)_A$ prediction with the observed values for the considered catchments.

In a second instance, a regional assessment for μ(Q), $\mu(Q)_D$, was provided through the regional scale evaluation of mean annual runoff from the annual soil water balance (Cannarozzo et al., 2009; Viola et al., 2017). In particular for the investigated region, Rossi and Silvagni (1980) proposed the following equation for regional prediction of mean annual runoff μ(D):

$$\mu(D)^{1/3} = -20.08 + 11.09 \cdot \log(P) - 5.19 \cdot \log(T) \tag{7}$$

where P and T are respectively the mean annual precipitation and the mean annual air temperature. μ(D) was converted into $\mu(Q)_D$ by means of catchment area and compared in Fig. 10 right panel with the observed values for the considered catchments.

For what concerns instead the BFI, in a previous paper (Longobardi and Villani, 2008) the authors showed the results of a regional prediction framework for BFI estimation at ungauged sites for the region under investigation. In particular, it was demonstrated that a simple partition of catchment area A into permeable areas (A_{perm}) and impervious areas can be used to define a permeability index PI, the ratio A_{perm}/A, which represent the independent variable for the analysed area for the BFI estimation:

$$BFI = BFI_{perm} \cdot PI + BFI_{\min} \tag{8}$$

with BFI_{perm} and BFI_{min} least square regional regression parameters based on the discharge and catchment features data of the studied area. A 68 % explained variance was found for Eq. (8).

Taking into account the illustrated formulations, the regression models reported in Table 7 for the prediction of $\mu(Q_{95})$ resulted in the calibration and assessment provided in Table 10. Clearly, the use of both $\mu(Q)_A$ and $\mu(Q)_D$ for the regional scale description of μ(Q) led to the same performance.

For what concerns instead the $CV(Q_{95})$, as no relationships were found between the precipitation variability CV(P) and any of the available catchment attributes, only the simple regression equation, where the independent variable is the BFI, was recalibrated. Results are provided in Table 11.

The fully regional approach showed clearly different performance capacity compared to the prediction based on the observed hydrological variables but not significantly lower.

7. Conclusion

The environmental flow (EF) is a critical parameter called to balance the need to provide the worldwide growing population with reliable water supplies on one side and sustain, restore or maintain ecosystem services on the other side. Some of the estimation procedures take into account the natural variability of river flow by considering the intra-annual EF variability but the question of the deviation of the EF indices from the long term natural ranges is far from being fully addressed. In this context, the current research was framed to recommend methodologies for EFs and EFs inter-annual variability estimation and test how the recommendation for the most suitable method is influenced by the river basin characteristics, with particular reference to the geological and climate settings, known to be the main drivers of low flow conditions.

Regional relationship for the prediction of average EF $\mu(Q_{95})$ and EF inter-annual variability, $CV(Q_{95})$, were calibrated. They were based on hydrological variables and physical catchment attributes. In particular regional regression equations with two independent variables appeared the best prediction models for both $\mu(Q_{95})$ and $CV(Q_{95})$, with $\mu(Q_{95})$ strongly dependent on catchment area A and mean annual daily discharge μ(Q) and $CV(Q_{95})$ dependent on the BFI index and the coefficient of variation of the precipitation CV(P). It was showed that simple regression regional equations can be valid alternative to multiple regression equations, for both $\mu(Q_{95})$ and CV (Q_{95}), but it was necessary to group the catchments and provide a specific calibration for each group. For what concerns $\mu(Q_{95})$ the

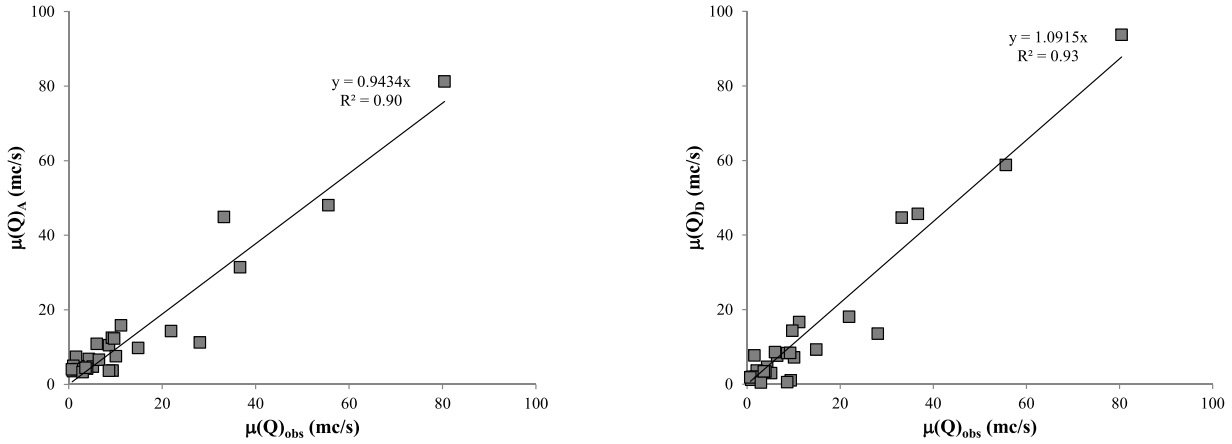

Fig. 10. Comparison between observed and regional estimations of mean annual daily discharge μ(Q)A (left panel) and μ(Q)D (right panel).

Table 10
μ(Q95) single and multiple regression models for the investigated region in a fully regional approach.

Regression model	r^2_{corr}	APE(%)	Valid for
$\mu(Q_{95}) = 1.53 + 0.0039*A$	0.79	−506.52	Whole region
$\mu(Q_{95}) = 1.64 + 0.004*A + 0.0015*P-0.094*T$	0.79	−513.70	Whole region
$\mu(Q_{95}) = -1.48 + 0.0044*A + 0.056*PI$	0.83	−111.66	Whole region
$\mu(Q_{95}) = \begin{cases} -0.608 + 0.044 * A \\ +0.988 + 0.18 * A \end{cases}$	0.88	−114.97	Whole region, with BFI < 60 % Whole region, with BFI > 60 %

Table 11
CV(Q95) single regression model for the investigated region in a fully regional approach.

Regression model	r^2_{corr}	APE(%)	Valid for
$CV(Q_{95}) = 0.52*PI\hat{}-1.28 + 0.0021$	0.35	−29.55	Whole region

group rule was based on the BFI index and the independent variable was set on the mean annual daily discharge μ(Q). For what concerns instead $CV(Q_{95})$ the group rule was based on the CV(P) index and the independent variable was set on the BFI index.

The regional regression equations for $\mu(Q_{95})$ and $CV(Q_{95})$ prediction were in the end re-calibrated to provide a fully regional approach, simply based on physical catchment attributes, also embedding the impact of hydrological variables which necessarily originate from continuous observations, unavailable for ungauged sites. The fully regional approach showed clearly different performance capacity compared to the prediction based on the observed hydrological variables but not significantly lower.

Operationally, if hydrometric data are available in the region and it is possible to establish a relationship between μ(Q) and A, from this it is possible to estimate the value of μ(Q) and then calculate the average value of EF, $\mu(Q_{95})$. From the geological characteristics it will similarly be possible to estimate the value of $CV(Q_{95})$ and from this, as $\mu(Q_{95})$ is known, the standard deviation of Q_{95} and therefore the maximum and minimum expect EF values can be assessed. If hydrometric data are not available in the region, it is possible to use only climatic data and geological characteristics to make the same estimates, however with reduced performance as typically occurs in regional analyses.

The findings related to the inter-annual variability of EFs on one side confirmed the importance to account for such feature and on the other side encourage a feasible identification of the systems mostly affected by the EF variability. Large deviations of EF from long term averages were observed for the region under investigation indeed. By the reconstruction of annual flow duration curves, it was found that in about 32 % of cases, the minimum observed value of Q_{95} was lower than the lower boundary of a 5% significance level confidence interval. The vulnerability of those systems seemed to arise from a combination of both precipitation variability (CV(P)) and geological features (BFI). The EF inter-annual variability was more sensitive for catchments featured by large CV(P), but the difference were mostly evident in the case of low BFI values. In a global environmental change and sustainability perspective, a conceptual modelling approach able to mimic the hydrological behaviour of those system under climate scenario characterized by more detailed climate variability indices would represent an undeniable useful tool to inform water resources managers about the best management practices to be adopted for a more rationale freshwater utilization.

CRediT authorship contribution statement

A. Longobardi: Conceptualization, Methodology, Investigation, Formal analysis, Writing - original draft, Writing - review & editing. **P. Villani:** Conceptualization, Methodology, Writing - original draft, Writing - review & editing.

Declaration of Competing Interest

The authors report no declarations of interest.

Acknowledgments

The authors will to thank anonymous reviewers for their helpful comments which resulted in an improved manuscript. The authors gratefully acknowledge funding support provided through the Instruction, University and Research Italian Ministry (MIUR) under the grant ORSA164189 and ORSA154528.

Appendix A. Supplementary data

Supplementary material related to this article can be found, in the online version, at doi:https://doi.org/10.1016/j.ejrh.2020.100764.

References

Acreman, M.C., Dunbar, M.J., 2004. Defining environmental river flow requirements – a review. Hydrol. Earth Syst. Sci. 8, 861–876.

Acreman, M.C., Ferguson, A.J.D., 2010. Environmental flows and the European water framework directive freshwater. Biology 55, 32–48.

Alcázar, J., Palau, A., 2010. Establishing environmental flow regimes in a Mediterranean watershed based on a regional classification. J. Hydrol. 388 (1–2), 41–51.

Cannarozzo, M., Noto, L.V., Viola, F., La Loggia, G., 2009. Annual runoff regional frequency analysis in Sicily. Phys. Chem. Earth Parts A/B/C 34 (10–12), 679–687.

Castellarin, A., Camorani, G., Brath, A., 2007. Predicting annual and long-term flow-duration curves in ungauged basins. Adv. Water Resour. 30, 937–953.

Cheng, L., Yaeger, M., Viglione, A., Coopersmith, E., Ye, S., Sivapalan, M., 2012. Exploring the physical controls of regional patterns of flow duration curves –part 1: insights from statistical analyses. Hydrol. Earth Syst. Sci. 16, 4435–4446.

Claps, P., Fiorentino, M., 1997. Probabilistic flow duration curves for use in environmental planning and management. In: Harmancioglu, N.B., Alpaslan, M.N., Ozkul, S.D., Singh, V.P. (Eds.), Integrated Approach to Environmental Data Management Systems. NATO ASI Series (Series: 2: Environment), vol. 31. Springer, Dordrecht, pp. 255–266.

Gleeson, T., Wada, Y., Bierkens, M.F., van Beek, L.P., 2012. Water balance of global aquifers revealed by groundwater footprint. Nature 488, 197–200.

Hanasaki, N., Kanae, S., Oki, T., Masuda, K., Motoya, K., Shirakawa, N., Shen, Y., Tanaka, K., 2008. An integrated model for the assessment of global water resources – part 1: model description and input meteorological forcing. Hydrol. Earth Syst. Sci. 12, 1007–1025.

Kobold, M., Brilly, M., 1994. Low flow discharge analysis in Slovenia. In: Seuna, P., Gustard, A., Arnell, N.W., Cole, G.A. (Eds.), FRIEND: Flow Regimes from International Experimental and Network Data. IAHS Publ. no. 221, pp. 119–131. Proc. Braunschweig Symp., October 1993.

Laaha, G., Blöschl, G., 2007. A national low flow estimation procedure for Austria. Hydrol. Sci. J. 52 (4), 625–644.

Lin, K., Lin, Y., Xu, Y., Chen, X., Chen, L., Singh, V.P., 2017. Inter- and intra- annual environmental flow alteration and its implication in the Pearl River Delta, South China. J. Hydro-Environ. Res. 15, 27–40.

Longobardi, A., Mautone, M., 2015. Trend analysis of annual and seasonal air, Engineering Geology for Society and Territory - Volume 3: River Basins. Reserv. Sedim. Water Resour. 501–504.

Longobardi, A., Van Loon, A.F., 2018. Assessing baseflow index vulnerability to variation in dry spell length for a range of catchment and climate properties. Hydrol. Process. 32 (16), 2496–2509.

Longobardi, A., Villani, P., 2008. Baseflow index regionalization analysis in a Mediterranean area and data scarcity context: role of the catchment permeability index. J. Hydrol. 355 (1–4), 63–75.

Longobardi, A., Villani, P., 2010. Trend analysis of annual and seasonal rainfall time series in the Mediterranean area. Int. J. Climatol. 30 (10), 1538–1546.

Longobardi, A., Villani, P., 2013. A statistical, parsimonious, empirical framework for regional flow duration curve shape prediction in high permeability Mediterranean region. J. Hydrol. 507, 174–185.

Longobardi, A., Buttafuoco, G., Caloiero, T., Coscarelli, R., 2016. Spatial and temporal distribution of precipitation in a Mediterranean area (southern Italy). Environ. Earth Sci. 75 (3), 189, 1-20.

Mohamoud, Y.M., 2008. Prediction of daily flow duration curves and streamflow for ungauged catchments using regional flow duration curves. Hydrol. Sci. J. 53, 706–724.

Nyika, J., 2017. Situational analysis of Nairobi river basin (NRB). Water Pract. Technol. 12 (3), 589–603.

Olsen, M., Troldborg, L., Henriksen, H.J., Conallin, J., Refsgaard, J.C., Boegh, E., 2013. Evaluation of a typical hydrological model in relation to environmental flows. J. Hydrol. 507, 52–62.

Opdyke, D.R., Oborny, E.L., Vaugh, S.K., Mayes, K.B., 2014. Texas environmental flow standards and the hydrology-based environmental flow regime methodology. Hydrol. Sci. J. 59 (3–4), 820–830.

Palau, A., Alcazar, J., 2012. The basic flow method for incorporating flow variability in environmental flows. River Res. Appl. 28, 93–102.

Papadaki, C., Soulis, K., Ntoanidis, L., Zogaris, S., Dercas, N., Dimitriou, E., 2017. Comparative assessment of environmental flow estimation methods in a Mediterranean Mountain River. Environ. Manage. 60, 280–292.

Pastor, A.V., Ludwig, F., Biemans, H., Hoff, H., Kabat, P., 2014. Accounting for environmental flow requirements in global water assessments. Hydrol. Earth Syst. Sci. 18, 5041–5059.

Peñas, F.J., Juanes, J.A., Álvarez-Cabria, M., Álvarez, C., García, A., Puente, A., Barquín, J., 2014. Integration of hydrological and habitat simulation methods to define minimum environmental flows at the basin scale. Water Environ. J. 28, 252–260.

Peres, D.J., Cancelliere, A., 2016. Environmental flow assessment based on different metrics of hydrological alteration. Water Resour. Manage. 30, 5799–5817.

Ren, K., Huang, S., Huang, Q., Wang, H., Leng, G., 2018. Environmental flow assessment considering inter and intra-annual streamflow variability under the context of non-stationarity. Water 10, 1737.

Richter, B.D., Baumgartner, J.V., Powell, J., Braun, D.P., 1996. A method for assessing hydrologic alteration within ecosystems. Conserv. Biol. 10 (4), 1163–1174.

Rossi, F., Silvagni, G., 1980. Analysis of annual runoff series. In: Third International Symposium on Stochastic Hydraulics, 5–7 August. Tokio, Japan.

Smakhtin, V.Y., Hughes, D.A., Creuse-Naudin, E., 1997. Regionalization of daily flow characteristics in part of the Eastern Cape, South Africa. Hydrol. Sci. J. 42 (6), 919–936.

Tessmann, S., 1980. Environmental Assessment, Technical Appendix E in Environmental Use Sector Reconnaissance Elements of the Western Dakotas Region of South Dakota Study. South Dakota State University, Water Resources Institute, South Dakota State University, Brookings, South Dakota.

Tharme, R.E., 2003. Global perspective on environmental flow assessment: emerging trends in the development and application of environmental flow methodologies for rivers. River Res. Appl. 19, 397–441.

Vezza, P., Comoglio, C., Rosso, M., Viglione, A., 2010. Low flows regionalization in North-Western Italy. Water Resour. Manage. 24, 4049–4074.

Viola, F., Caracciolo, D., Forestieri, A., Pumo, D., Noto, L.V., 2017. Annual runoff assessment in arid and semiarid Mediterranean watersheds under the Budyko's framework. Hydrol. Process. 31 (10).

World Meteorological Organization, 2019. Guidance on Environmental Flows Integrating E-Flow Science with Fluvial Geomorphology to Maintain Ecosystem Services, WMO-No. 1235.